



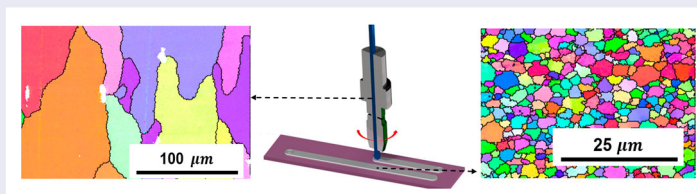
Additive friction stir deposition: a deformation processing route to metal additive manufacturing

Hang Z. Yu ^a and Rajiv S. Mishra ^{b,c}

^aDepartment of Materials Science and Engineering, Virginia Tech, Blacksburg, VA, USA; ^bCenter for Friction Stir Processing, Department of Materials Science and Engineering, University of North Texas, Denton, TX, USA; ^cAdvanced Materials and Manufacturing Processes Institute, University of North Texas, Denton, TX, USA

ABSTRACT

As the forging counterpart of fusion-based additive processes, additive friction stir deposition offers a solid-state deformation processing route to metal additive manufacturing, in which every voxel of the feed material undergoes severe plastic deformation at elevated temperatures. In this perspective article, we outline its key advantages, e.g. rendering fully-dense material in the as-printed state with fine, equiaxed microstructures, identify its niche engineering uses, and point out future research needs in process physics and materials innovation. We argue that additive friction stir deposition will evolve into a major additive manufacturing solution for industries that require high load-bearing capacity with minimal post-processing.



IMPACT STATEMENT

This paper delineates additive friction stir deposition, which offers a solid-state deformation processing route to metal additive manufacturing and renders fully-dense material with fine, equiaxed microstructures in the as-printed state.

ARTICLE HISTORY

Received 21 October 2020

KEYWORDS

Additive manufacturing; deformation processing; additive friction stir deposition; equiaxed microstructure; repair and recycling

1. Introduction

Classical metal manufacturing and joining involve two distinct routes: one is based on melting and solidification; the other leverages plastic deformation. To fabricate a metallic component with the desired geometry, a materials engineer may heat and melt the metal, pour it into a mold with a pre-defined shape, and let it solidify inside the mold by cooling. This is the casting process [1]. Alternatively, one may press or hammer the metal into the desired shape while the metal remains in the solid-state. This is the forging process [2]. While casting is more capable of producing large and complex shapes, forging leads to improved mechanical properties, such as better ductility, higher yield and tensile strengths, and substantially longer fatigue lifetime. To join two metal workpieces, a materials engineer may employ arc [3], gas

[4], resistance [5], or laser welding [6] and create the metallurgical bonds via the liquid bonding mechanism. These processes are classified as fusion welding [7,8]. Alternatively, one may employ diffusion [9], ultrasonic [10], explosion [11,12], friction or friction stir welding [13] to force the materials in intimate contact and create the metallurgical bonds via diffusion of the interface atoms. These processes are classified as solid-state welding [14]. While fusion welding is more flexible in terms of the primary shapes of the components, solid-state welding leads to comparatively lower levels of distortion and residual stresses, a narrower heat-affected zone, and significant forging action in the heat and deformation zone [8].

Just like conventional manufacturing and joining, additive manufacturing of metals can also be

implemented via two routes: solidification from the molten state and plastic deformation. The former category is termed fusion-based or beam-based additive manufacturing, including powder bed fusion and directed energy deposition [15]. The feedstock powders, regardless of being pre-deposited to form a powder bed or delivered by nozzles, are melted by the energy of either a laser or an electron beam [16,17]. As the beam moves away, the subsequent molten pool cools down and solidifies, forming a track of solidified material corresponding to the scanning path of the beam. As in casting and fusion welding, fusion-based metal additive manufacturing inevitably compromises the control of porosity, residual stress, and hot cracking due to the liquid phase bonding mechanism [18,19]. These issues are especially worsened by the small molten pool size, large thermal gradient, and high cooling rate [20]. Moreover, because textured, columnar grain structures naturally form along the build direction [21], microstructure control has been a recurring challenge despite the advances in recent years [22–24].

To fundamentally address the quality control issues inherent to fusion-based additive manufacturing, we must resort to the deformation processing route. Inspired by solid-state welding, several deformation-based metal additive manufacturing approaches have emerged during the last few years [25]. These include ultrasonic additive manufacturing [26,27], cold spray additive manufacturing [28,29], and additive friction stir deposition (AFSD) [30,31]. Without material melting, these approaches exploit deformation bonding to implement layer adhesion via ultrasonic vibration, particle impact, and friction stirring, respectively. Compared to ultrasonic and cold spray additive manufacturing, AFSD stands out as a particularly promising approach. First, ultrasonic additive manufacturing is a hybrid technology based on initial ultrasonic welding of foils followed by CNC (computer numerical control) machining, whereas AFSD is a freeform fabrication process that enables printing at specific locations. Second, cold spray additive manufacturing often leads to incompletely bonded interfaces between particles, resulting in porosity and micro-cracks [32,33]; in contrast, AFSD typically renders fully-dense parts in the as-printed state [30,34]. Third, while ultrasonic additive manufacturing, cold spray additive manufacturing, and AFSD are all based on deformation bonding, the former two only involve local plastic deformation around the interface or particle contact regions. In AFSD, the plastic deformation is global: every voxel of the feed material undergoes severe plastic deformation at elevated temperatures [25]. This gives rise to a uniform recrystallized microstructure with minimal, if any, internal defects. Thanks to its thermomechanical

processing style, AFSD is by far the only metal additive manufacturing process that can lead to wrought or comparable mechanical properties in the as-printed state [25,35].

As the forging counterpart of fusion-based additive manufacturing processes, AFSD has great potential to thrive in the aerospace, automotive, and defensive industries and deserves special attention. In this perspective article, we provide a state-of-the-art overview of this process and the related research efforts, with a focus on its salient advantages over fusion-based additive manufacturing and niche engineering applications. We show that there are plenty of research opportunities in the fundamental realms, especially in process physics and materials innovation. Their realization is vital for AFSD to make a strong impact in the metal additive manufacturing community.

2. Notable characteristics of AFSD

2.1. Printing by deforming

At first glance, the mechanical setup of an AFSD machine approximately resembles the configuration of fused deposition modeling, which simply uses heating and compression to enable thermoplastic printing. However, deformation of metallic feed material and creation of material-substrate bonding require a much more efficient thermomechanical processing strategy. This is why in AFSD the friction stir principle is leveraged. By combining this with a vertical material feeding mechanism, metals can be printed through rapid heating and deformation.

In AFSD, a metal rod rapidly rotates as it is delivered through the tool head and starts to generate frictional heat as it contacts the substrate. The feed material then increases in temperature, yields, and extrudes to fill the space between the substrate and the rotating tool head. The bottom surface of the tool head has two functions. First, it controls the layer thickness by providing a vertical constraint. Second, its rotation further smears and shears the deposited material to ensure good print quality with no porosity. Good interface bonding is achieved thanks to the co-deformation and mixing of the deposited material and substrate surface [36]. Similar to fused deposition modeling, the in-plane motion of the tool head relative to the substrate controls the material pattern in each layer, and 3D parts are readily printed in a layer-by-layer fashion. Figure 1 illustrates the AFSD principle with a comparison to alternative additive processes, including ultrasonic additive manufacturing, cold spray additive manufacturing, and powder bed fusion. We note that in addition to solid rod, powder feedstock can be used as

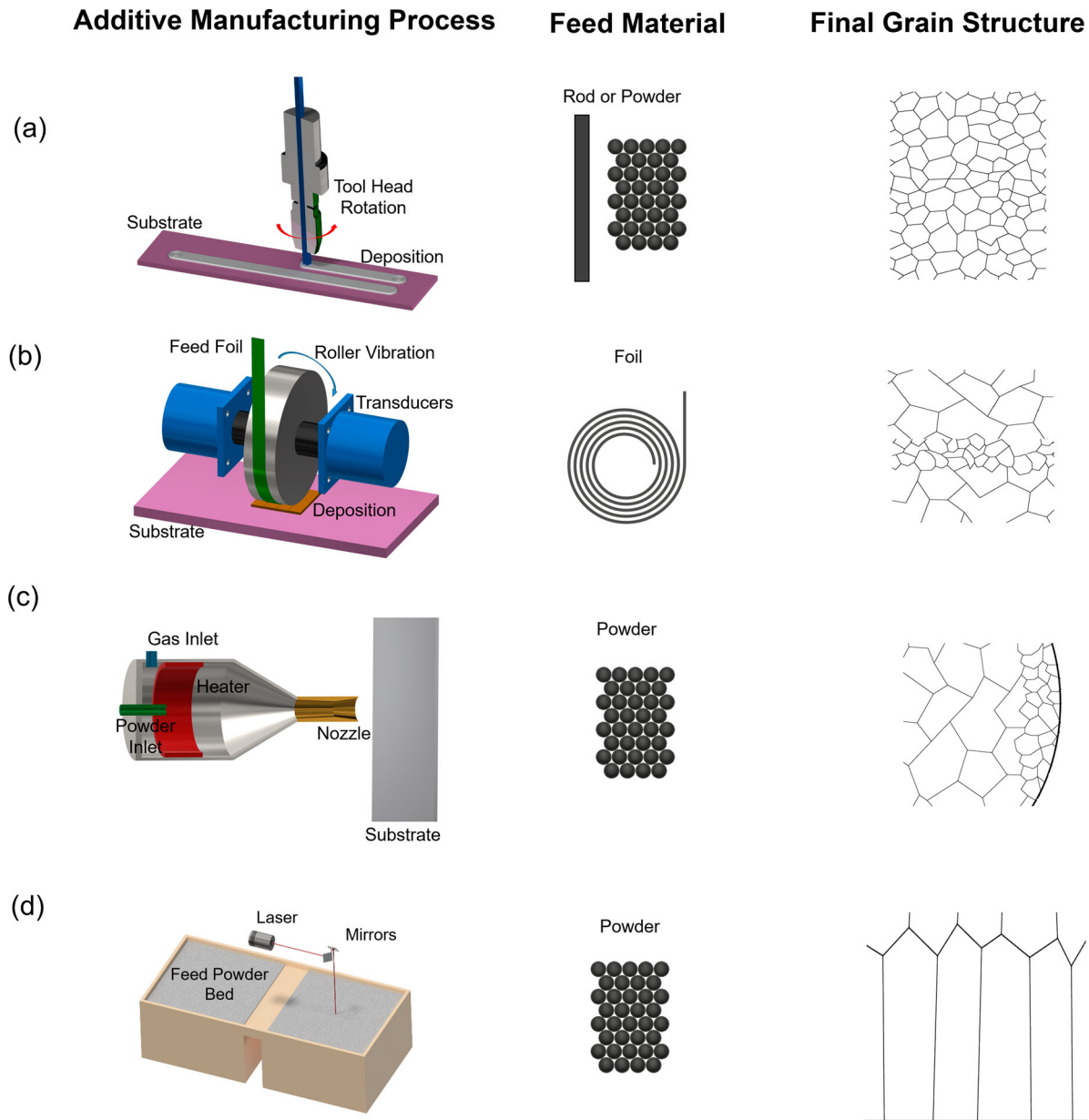


Figure 1. Comparisons of the machine configuration, the form of feed material, and the final grain structure among different additive manufacturing processes: (a) additive friction stir deposition, (b) ultrasonic additive manufacturing, (c) cold spray additive manufacturing, and (d) selective laser melting.

the feed material in AFSD, which involves a different tool head design based on an auger conveyor [34,37].

2.2. Salient advantages over fusion-based additive manufacturing

With the material addition and bonding implemented via severe plastic deformation at elevated temperatures, AFSD offers a deformation processing route to metal additive manufacturing. Intuitively, its advantages over fusion-based additive manufacturing are analogous to that in forging versus casting and in solid-state welding versus fusion welding. As elaborated below, these

advantages are particularly rooted in the absence of melting and the benefits of thermomechanical processing.

2.2.1. Porosity

In fusion-based metal additive manufacturing, process-induced porosity is a common type of defect [38]. When the applied energy via laser or electron beam is insufficient to fully melt the material, ‘lack of fusion’ results in the formation of pores [39]. When the applied energy is excessively high, porosity can arise due to spatter ejection [40]. During solidification of alloys, when the constituents with low melting temperatures are rejected

at the liquid–solid interface, thin liquid regions can form between the solidified dendrites. The solidification shrinkage then leads to hot tearing or hot cracking—an effect profound in non-weldable alloys, such as high-strength aluminum alloys [22]. The powder feedstock may also contain pores because of the gas entrapment during gas atomization, which may be transferred to the printed parts [41].

AFSD, in contrast, can render fully-dense metal parts in the as-printed state. Without melting, there are no concerns regarding the aforementioned solidification-induced porosity. More importantly, the deformation state in AFSD is predominantly characterized by compression and shear, which effectively eliminates potential internal defects during printing. Even if the feed material is not fully dense, the as-printed material can be free of porosity thanks to the intense material deformation and flow under the tool head [34,37].

2.2.2. Microstructure

The microstructure resulting from fusion-based metal additive manufacturing is characterized by highly oriented, columnar grains as a result of epitaxial solidification. In cubic metals, for instance, (100) is the fast growth direction during solidification, so the as-printed material frequently exhibits a strong (100) texture along the build direction [42,43]. To promote equiaxed microstructures for structural applications, the process parameters (e.g. laser power and scanning speed) need to be carefully adjusted [44]. The goal is to enhance the relative dominance of solidification velocity (R) over thermal gradient (G) so that undercooling is sufficiently large to trigger nucleation inside the molten pool [45,46]. As a notable breakthrough, the addition of nanoparticles to the feedstock is shown to be a viable solution for microstructure control. These nanoparticles survive in the molten pool and have their surfaces serve as the heterogeneous nucleation sites [22,47,48]. As illustrated in Figure 2(a), this effectively promotes the formation of equiaxed grains while preventing hot cracking issues.

To compare, AFSD characteristically leads to refined, equiaxed microstructures due to its thermomechanical processing nature [35,36,49]. Because of the friction stir principle, the deposited material is severely and rapidly deformed with the peak temperature above half of the melting temperature [50]. This leads to dynamic microstructure evolution [51], which can be divided into discontinuous and continuous types of dynamic recrystallization depending on the characteristic physical variables in processing—e.g. peak temperature and strain rate—as well as the intrinsic material properties, such as the stacking fault energy [52].

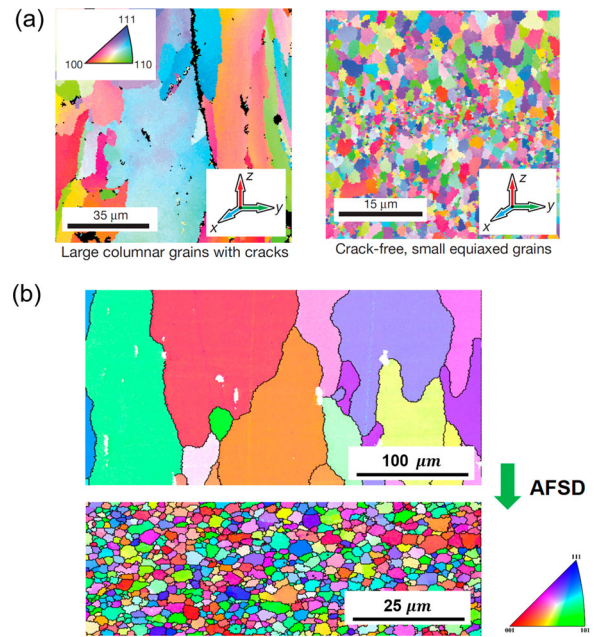


Figure 2. Characteristic microstructures by fusion-based additive manufacturing and AFSD. (a) The microstructure resulting from selective laser melting of AA7075 (left) without and (right) with the addition of Zr nanoparticles. Images reproduced with permission from reference [22]. (b) The microstructure of (top) AA2024 feed-rod by drawing and (bottom) printed AA2024 by AFSD. Images reproduced with permission from reference [36].

In materials with high stacking fault energy, such as aluminum and its alloys, AFSD commonly leads to continuous dynamic recrystallization, which proceeds by extensive dynamic recovery, subgrain formation, and a gradual increase of the misorientation angle with the strain [53]. Both geometric dynamic recrystallization and progressive lattice rotation belong to this category. In materials of lower stacking fault energy, discontinuous dynamic recrystallization can be more significant. This involves the growth of small, dislocation-free grains by high-angle grain boundaries sweeping through the deformed matrix. The continuous and discontinuous dynamic recrystallization processes cause the formation of equiaxed grains with a significantly reduced size [54]. For example, feedstock made from aluminum alloys (e.g. 2xxx [36,55], 6xxx [31], and 7xxx [49,56]) with a coarse microstructure (grain size ~ 100 – $200 \mu\text{m}$) may have their grain size reduced to 1 – $5 \mu\text{m}$ after AFSD. Figure 2(b) shows an example for AFSD of AA2024, with a comparison of the microstructure before and after printing.

2.2.3. Energy consumption, cost, and convenience

Fusion-based additive manufacturing requires the use of high-energy beam sources to fully melt the feed material rapidly [57,58]. The high heat input inevitably causes large thermal gradients around the molten pool

and therefore high residual stresses. This makes post-processing, such as annealing or hot isostatic pressing, necessary to alleviate the stress level and distortion in the as-printed parts [59,60]. Without melting and solidification, AFSD provides a low-energy pathway to additive manufacturing with reduced heat input and residual stresses. In addition to less energy consumption, such a capability allows for additive manufacturing of ultra-large structures without the concern of significant distortion. For example, it has been recently demonstrated that AFSD can print aluminum ring structures with a diameter of 3.05 meters [61].

Fusion-based additive manufacturing relies on the use of expensive laser or electron beams, while AFSD is based on simple mechanical principles with the hardware partially resembling a milling machine. Fusion-based additive manufacturing is often strict on the feed material attributes, e.g. the powder shape and size, to ensure good print quality. In AFSD, any solid bar of arbitrary compositions can be used as the feed material; to print cast or wrought engineering alloys, one can just machine the bar geometry and insert that into the tool head. The non-weldable alloys are also readily printed using AFSD; there is no need to carefully change the processing parameters or incorporate nanoparticles to prevent hot cracking.

While we highlight the advantages of AFSD over fusion-based additive manufacturing, it is important to note its limitations. In AFSD, the geometrical precision in the build direction, which is characterized by the layer thickness, is well controlled by the spacing between the tool head and substrate. However, the precision of in-plane dimensions relies on the material deformation and flow under the tool head. If the tool head drives sufficient material rotation, smooth edges arise along the deposition track, like the case in AFSD of AA6061 [50]. Otherwise, rough edges may form due to the ‘flash’ during material flow. This is why AFSD is better termed as near-net-shaping additive manufacturing. The current tooling size results in wide deposition tracks on the order of centimeters, allowing for high build rates and good scalability. That being said, this also suggests limits on the smallest attainable feature size [30]. Overall, rather than producing complex geometries with small feature sizes, AFSD is better suited for large-scale additive manufacturing in which structural integrity is a must.

3. Where is the market?

What most distinguishes AFSD from other metal additive manufacturing processes is the fully-dense material in the as-printed state along with fine, equiaxed microstructures and excellent mechanical properties. The most

promising market for AFSD thus lies in where excellent mechanical properties are highly desired and minimal post-processing heat treatment is preferred. In terms of materials, AFSD has particular advantages in processing and manufacturing of high-strength aluminum alloys that suffer from hot cracking issues in fusion-based additive manufacturing [36,49,55,56].

One niche application of AFSD is the structural repair of components for the aerospace and defense industries, in which load-bearing components may suffer from corrosion, wear, or other damages. Griffiths *et al.* [56] explored the through-hole and groove filling of AA7075 plates and showed that AFSD was effective at filling the entire volume. Sufficient mixing was observed between the deposited material and the sidewall of the feature; as a result, the interface was indiscernible with a gradual change in microstructure. In that preliminary investigation, no optimization strategy was employed for process parameters and the scanning path, and inadequate repair quality was sometimes observed in deeper portions of the filling. In the on-going work by the same group of authors, such defects are shown to be largely eliminated by improving the repair strategy, e.g. by tuning the tool head rotation rate and dwell time. The repaired 7xxx Al coupons (after removing the excess deposited material from AFSD) exhibit decent static and fatigue performance.

Another unique area for AFSD to thrive is solid-state material recycling, which may be combined with additive manufacturing or cladding. Because of the intense material deformation and flow, AFSD has a high degree of tolerance for the feed material quality. Even if the feed material is not fully dense or contains impurities such as oxides, the as-printed material may still render good mechanical properties. Jordon *et al.* [37] machined an aluminum alloy 5083 plate to produce discontinuous chips and performed AFSD using an auger feed system. The as-printed material was shown to be fully-dense and exhibited good ductility with an 18% elongation. Compared to the wrought alloy of AA5083, the yield strength was reduced but the ultimate tensile strength was increased due to significant strain hardening. Figure 3 provides examples of AFSD applications in repair and recycling.

AFSD can also be used for selective area reinforcement for large-scale, thin components, such as automotive panels. Hartley *et al.* [62] showed that for thin automotive 6xxx Al (1.4 mm thick), high-quality cladding of a comparable thickness could be achieved without local buckling, wrinkling, or damage in the sheet metal. The reinforced structure (i.e. cladding plus sheet metal) exhibited a good combination of strength and ductility while significantly improving the bending stiffness. There was no

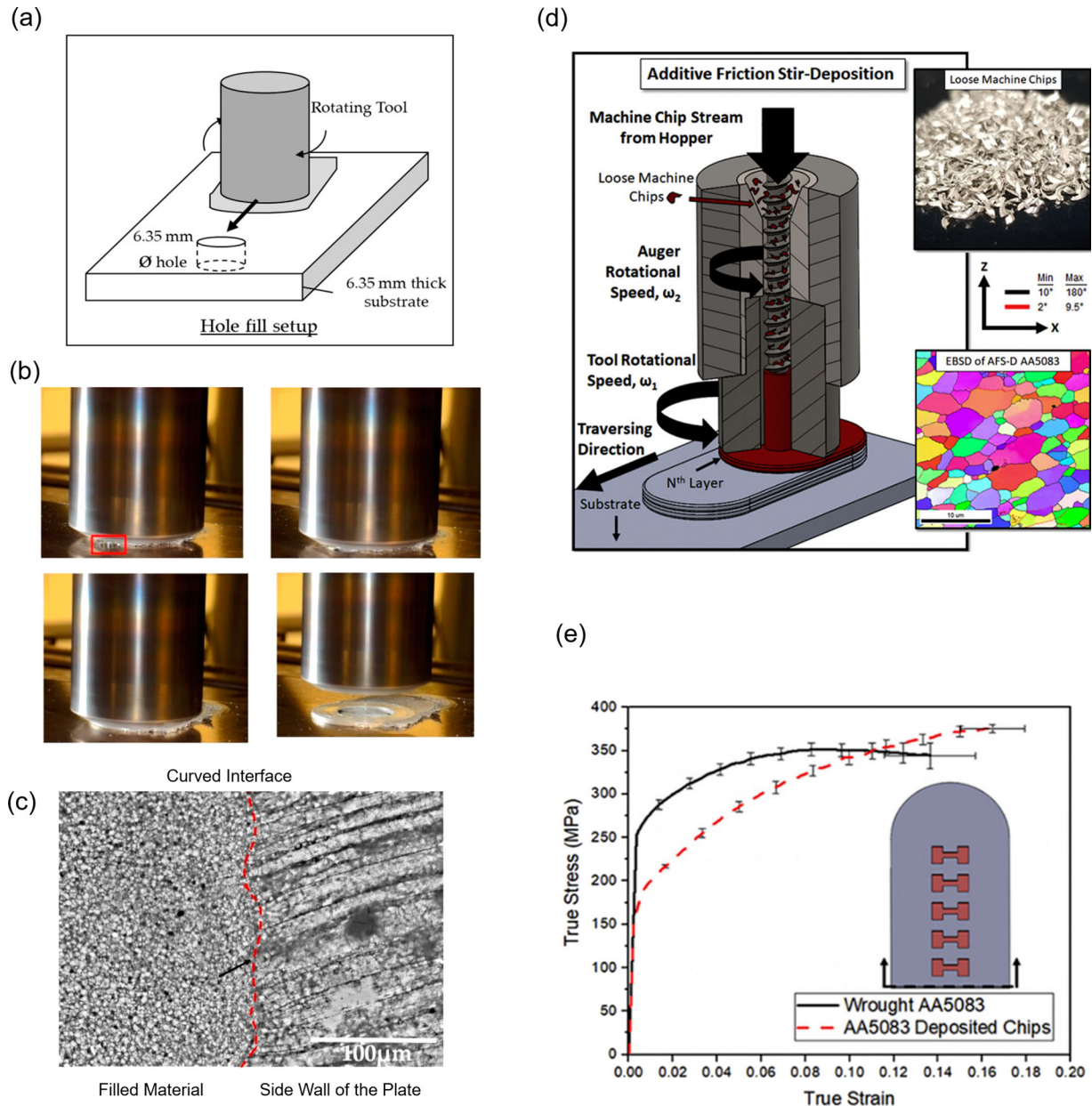


Figure 3. Niche engineering applications for AFSD: (a)–(c) repair and (d)–(e) recycling. (a) A sketch and (b) snapshots of the hole filling process for an AA7075 plate using AFSD. (c) A micrograph of the repair region showing a curved interface between a fine, equiaxed microstructure (filled material) and a rolling microstructure (side wall). Images reproduced with permission from reference [56]. (d) Illustration of the recycling process using AFSD. (e) Tensile properties of the printed AA5083 versus the wrought AA5083. Images reproduced with permission from reference [37].

sign of a sharp interface even after tensile failure, suggesting good mixing between the cladding and substrate. This point was also supported by the microstructural analysis, which showed a uniform grain structure across the nominal interface. Thanks to the absence of melting, the residual stress arising from AFSD was found to be low; the equivalent thermal strain at the interface was estimated to be only a fraction of the elastic limit of the material.

4. Path to impact: opportunities for future research

Despite the great promise for metal additive manufacturing, AFSD has not yet made a significant impact on the industry and academia. This is in part because it is a new additive process; not a lot of researchers or industry practitioners are aware of its unique advantages. More notably, the study on AFSD is only at an

entry-level, so the knowledge of the underlying process physics and materials science is fairly shallow. On the *process* side, tactics have remained elusive for controlling the strain, strain rate, and peak temperature in AFSD due to a lack of understanding of the material deformation, interface contact, and heat generation processes. On the *material* side, the thermomechanical processing characteristics of AFSD and its freeform fabrication capability unlock the freedom for material innovation across multiple length scales, but this capacity cannot be exploited without strategic control of grain size, grain boundary type, texture, and phase fraction in the as-printed alloys.

We argue that the path to impact lies in the fundamentals: widespread use of AFSD will be accelerated only when new advances are made in the *process* and *material* aspects. This offers plenty of research opportunities for materials scientists and engineers in the next phase, some of which are proposed as follows.

4.1. Towards an in-Depth understanding of the physics underlying the AFSD process

An in-depth understanding of the physics underlying the AFSD process calls for creative experimental efforts in the future. Like any additive manufacturing process, the thermal field and its evolution are vital in determining the print quality and microstructure development. Additionally, the material deformation history needs to be considered—AFSD is based on plastic deformation, and the thermal evolution and material deformation are fully coupled. For example, the constitutive mechanical properties that define the material response to external forces, such as stiffness, flow stress, strain hardening exponent, and dynamic viscosity, are all strongly temperature dependent and the latter three are strain rate dependent as well [63,64]. On the other hand, the material plastic deformation gives rise to energy dissipation and can be a major heat generation source along with the interface friction.

Because the fully coupled material deformation and heat generation govern the print quality and microstructure development, two basic questions must be answered for maximizing AFSD's impact:

- What is the typical thermal and deformation history of the deposited material during AFSD, i.e. temperature and strain as a function of time?
- How do the processing parameters in AFSD, such as tool head rotation rate (Ω) and travel velocity (V), determine the thermal and deformation history?

The thermal evolution is relatively straightforward to examine experimentally because the deposited material

lies on top of the substrate rather than being constrained by the surrounding material like the case of friction stir welding or processing. As shown in Figure 4, infrared imaging from the side can be used to monitor the temperature evolution in the deposited material. Garcia *et al.* [50] measured the peak temperature, exposure time, reheating rate, and cooling rate during AFSD of Al-Mg-Si and Cu under various conditions and found consistent physical trends. The peak temperature was found to be $\sim 50\%$ – 90% of the melting temperature, the exposure time is $\sim 10^1$ s, the reheating rate is $\sim 10^1$ – 10^2 K/second, and the natural cooling rate is $\sim 10^1$ K/second.

Based on the measured data, the authors also established empirical power-law relationships linking the peak temperature to the AFSD processing parameters. The quantitative differences of the peak temperature equations between Al-Mg-Si and Cu were attributed to their distinct material flow behavior, which was simultaneously captured via *in situ* surface imaging. Al-Mg-Si was seen to rotate under the tool head with intense deformation, whereas Cu remained stationary with the tool head-material interface showing a full slipping condition. This makes interface friction a dominant heat generation mechanism in the deposition zone of Cu; however, in Al-Mg-Si the heat generation is caused by both interface friction and volumetric energy dissipation from plastic deformation.

Compared to thermal monitoring, unraveling the material deformation history in AFSD is much more challenging given that the plastic deformation is rapid. While the work by Garcia *et al.* [50] was able to provide the material deformation and flow information on the exterior surface, little was revealed internally. This is not useful to understand the deformation history of the deposited material, i.e. how each voxel in the feed material deforms during initial material feeding and steady-state deposition. One feasible solution in the future is to place tracer material in the feed-rod and examine the tracer shape evolution at different steps of AFSD. From that, the deformation information of a given material voxel in the feed material can be recorded at incremental time steps, e.g. using X-ray computed tomography, and a full picture of the strain vs. time relationship can be eventually established. Such a time-resolved characterization approach has shown success in friction stir welding [65]. Real-time characterization of the tracer shape evolution may also be possible by leveraging the ultrafast X-ray imaging capabilities, e.g. in the Advanced Photon Source [66]. Another complementary strategy is to employ transparent feed material containing opaque particles [67]. Using high-speed optical imaging and digital image (or volume) correlation, the particle velocity field can be *in situ* measured to infer the strain rate of the

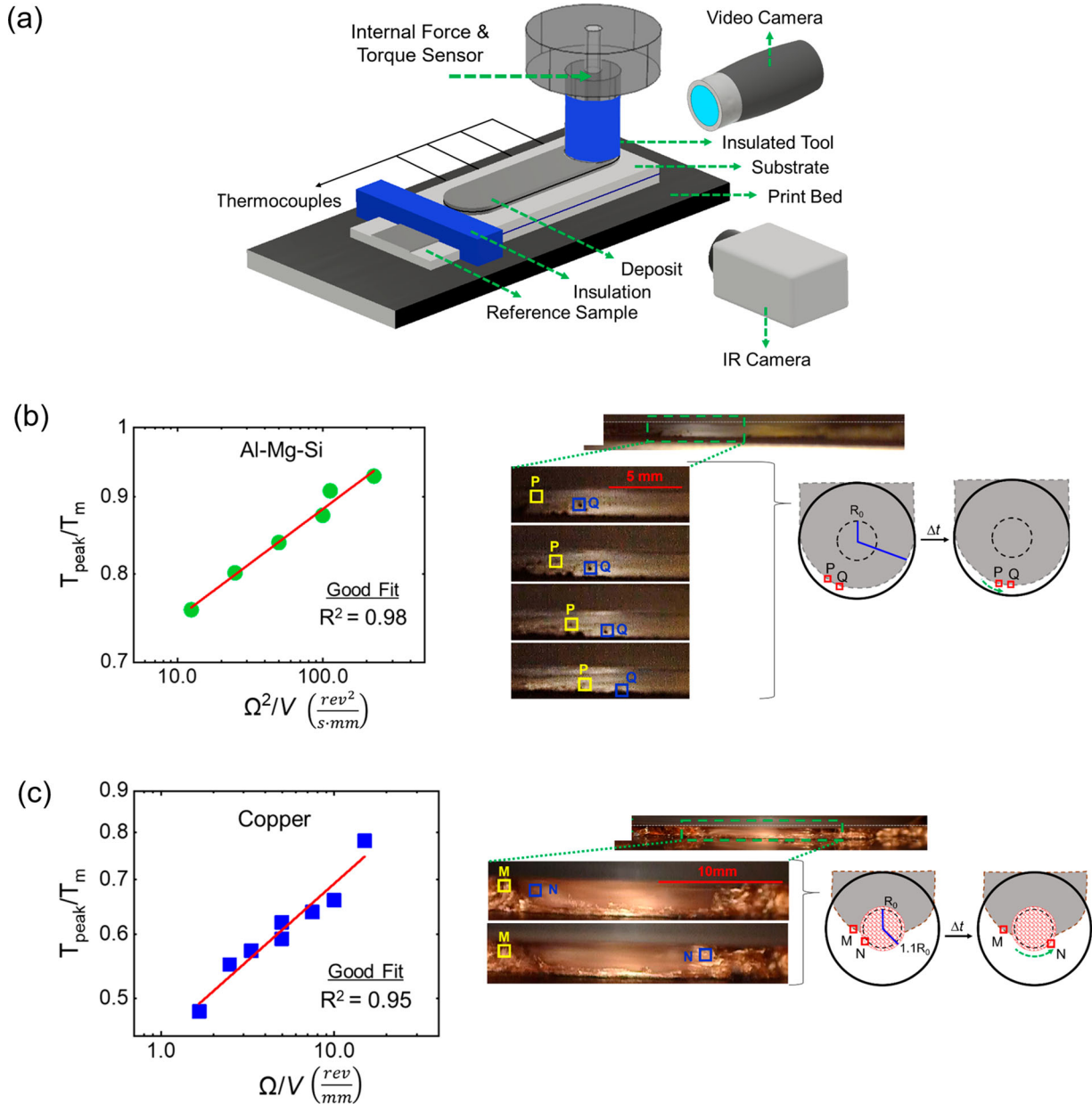


Figure 4. Thermal and material flow features of AFSD of Al-Mg-Si and Cu. (a) Illustration of the *in situ* monitoring system for AFSD. The correlation of peak temperature and processing parameters is found to be governed by the material flow behavior. A comparison is drawn between (b) Al-Mg-Si and (c) Cu. Images reproduced with permission from reference [50].

matrix material. While this only allows for using matrix material with desired optical and mechanical properties (e.g. ultra-high molecular weight polyethylene), the results can provide physical insights into the general deformation characteristics in AFSD.

4.2. Towards innovative materials research

AFSD unlocks unprecedented opportunities for materials innovation across multiple length scales. Characterized by a thermomechanical condition featuring rapid and large deformation, AFSD is accompanied by significant dynamic microstructure evolution. On the

microscopic level, it has plenty of room for tweaking the grain size, grain boundary type, and crystallographic texture. AFSD also enables site-specific printing. On the mesoscopic level, it can lead to location-dependent microstructure, phase, and properties along the print path, among deposition tracks, or across different layers. This offers new strategies for creating functionally graded materials, multi-layer structures, as well as heterogeneous and hierarchical microstructures.

4.2.1. On the microscopic level

Microstructure and grain boundary engineering is absolutely a bright direction for AFSD because dynamic

recrystallization results in a drastically refined, equiaxed microstructure. Depending on the cooling rate and material system, the microstructure may be in the ultra-fine or submicron grain regime, rendering considerable increases in the static strength especially if grain boundary strengthening and interfacial strengthening are the dominant strengthening mechanisms. An ultrafine grain structure may also be beneficial for high-cycle fatigue, wherein grain boundaries retard the crack propagation and lead to a crack closure effect. Evidence of this has been found in friction stir processed cast A356 alloy and 7075 Al alloy [68,69]. Microstructure control can be further extended to alloys that exhibit twinning-induced plasticity and transformation-induced plasticity. Severe plastic deformation processed nanocrystalline and ultra-fine grained alloys typically lack work hardening and the associated uniform elongation regime [70]. AFSD processing of low stacking fault energy alloys may activate the twinning or transformation-induced plasticity mechanisms to break down the strength-ductility trade-off paradigm [71,72].

For materials that evolve by continuous dynamic recrystallization, the deformation level in AFSD can be engineered to control the ratio between low and high angle grain boundaries as well as the magnitude and type of the shear texture [53,73,74]. The thermomechanical processing nature of AFSD allows for the alteration of intrinsic grain boundary properties too. By controlling the fractions of special grain boundaries, relative connectivity of the special and random grain boundaries, and the perfection of special boundaries compared to coincident site lattice, the resistance against sensitization [75] or hydrogen embrittlement [76] could be significantly improved in AFSD-printed austenitic stainless steels.

When printing two-phase alloys, the resultant fraction and spatial distribution of the secondary phase are sensitively dependent on the thermal and deformation history [77]. Starting from fully-aged, high-strength Al alloys, for example, AFSD can profoundly change the precipitate attributes, typically causing a decrease in strength and an increase in ductility [49]. The underlying phase and microstructure evolution are complex, possibly including multiple mechanisms that occur sequentially or simultaneously, such as dynamic recovery, dynamic recrystallization, particle stimulated nucleation, precipitate dissolution, dynamic precipitation, static precipitation, and particle coarsening [78–80]. The corresponding research opportunities are two-fold. First, empirical solutions are needed to achieve the desired precipitate attributes and mechanical properties in the as-printed state. This is critical for many engineering applications, such as repair and cladding, in which minimal post-heat treatment is preferred. Second, a fundamental theory is necessary to

predict the coupled dynamic microstructure and phase evolution under given thermomechanical conditions, especially those involving rapid, severe plastic deformation [77,81].

At this stage, only a limited number of alloy systems or matrix elements have been explored for AFSD. Recent results on friction stir processing of Mg [82,83] and Ti [84,85] alloys point to the ability of intense shear deformation processes to obtain strength-ductility combinations that are not possible through conventional thermomechanical processing routes. There is a very rich possibility of employing the ‘far-from-equilibrium’ AFSD process to reach unexplored regions for body-centered cubic elements and alloys. The body-centered cubic materials are well known for limited ductility; for many refractory elements, the ductile-brittle transition temperature is above the ambient temperature [86,87]. Two microstructural approaches that have been beneficial to enhance ductility are, (a) creating a very fine/ultrafine grained microstructure [88,89], and (b) creating a partially recrystallized microstructure [90]. The AFSD printing conditions may be manipulated to dramatically impact the microstructure for control of the strength-ductility synergy and ductile-to-brittle transition.

4.2.2. On the mesoscopic level

As illustrated in Figure 5, AFSD’s layer-by-layer manufacturing mode and excellent scalability provide new ways to fabricate bulk-scale mesostructured materials, such as functionally graded materials [91,92], and periodically structured and multi-layer structures [93,94]. If the mesostructured materials are characterized by a spatial distribution of chemical composition, feed-rods of different compositions can be employed for different layer deposition. If the mesostructured materials are characterized by a spatial distribution of microstructures or phase fractions, the thermomechanical condition during AFSD can be finely tuned as a function of the print location through process control.

The co-plastic deformation and mixing between the newly-deposited material and the layer underneath will lead to a diffuse interface with gradual changes in composition, microstructure, and phase fraction, rather than forming a sharp interface. Thanks to the short thermal cycle [50], there is a lower chance of forming undesired intermetallics at the interface. Even if brittle intermetallic phases form as a result of mechanical mixing, the imposed shear force and torque during AFSD would make them a globular shape with much less deterioration on the overall ductility [95,96].

Based on the strategy of fabricating multi-layer structures, AFSD can be used to fabricate an emerging class of

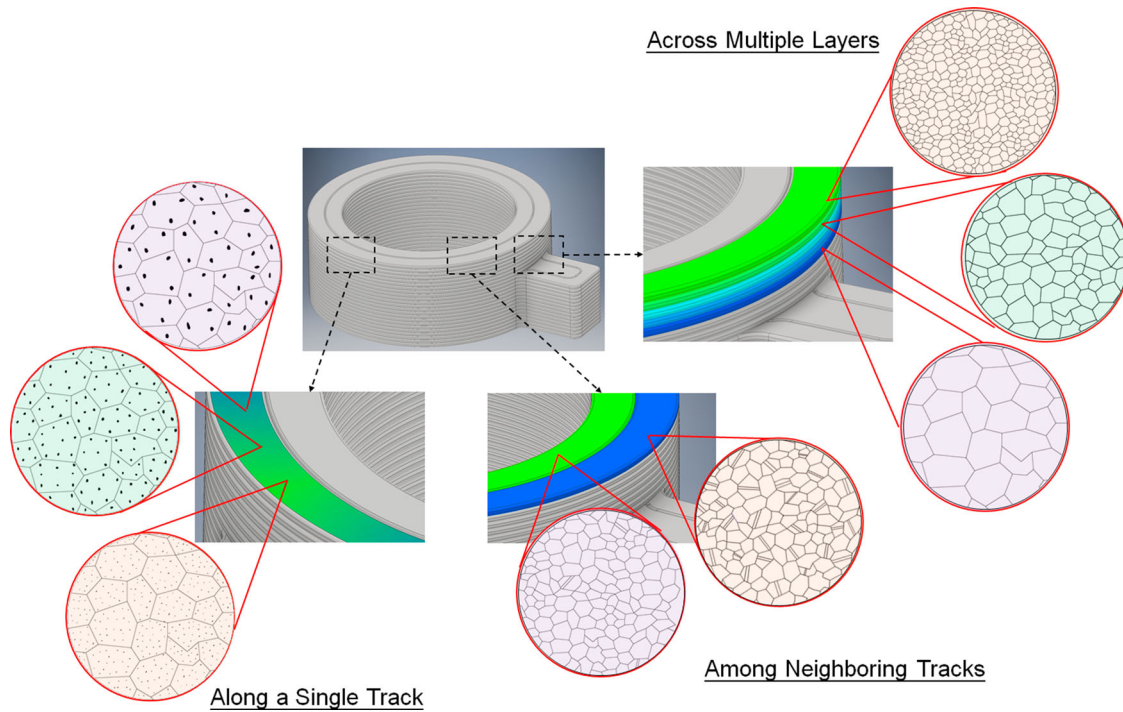


Figure 5. Opportunities of microstructure and mesostructure control unlocked by AFSD. On the microscopic level, examples are given for control of grain size, fraction of special grain boundaries, and precipitate attributes. On the mesoscopic level, examples are given for control along a single deposition track, among neighboring deposition tracks, and across multiple layers.

structural materials: the heterogeneous materials [97]. By exploiting the incompatible plastic deformation between the mesoscopic soft and hard zones, heterogeneous materials enable long-range back-stress development and hetero-deformation induced hardening [98,99], resulting in a good combination of strength and ductility. The AFSD process parameters and tool geometry can be used to adjust the morphology of the non-planar interface between soft and hard zones [36], which is known to be an important factor in determining the synergy of strength and ductility. Beyond that, structural and compositional engineering of the feed material may lead to new architected materials, which has been demonstrated in a few severe plastic deformation processes [100]. Overall, by integrating the mesoscale and microscale material innovation, AFSD has the potential to build hierarchical materials with controlled characteristic features across various length scales, from compositions, precipitate structures, grain structures, to the mesoscopic zones.

5. Summary

With the material undergoing severe plastic deformation at elevated temperatures, AFSD offers a deformation processing route to metal additive manufacturing. Notably, AFSD can lead to bulk-scale parts with good quality, fine equiaxed microstructure, and mechanical properties

comparable to wrought alloys even in the *as-printed* state. Renowned for high build rates and good scalability, the present machines are particularly advantageous for large-scale applications, whereas improvement of spatial resolution and geometric precision is a great area for the next-phase research and development. Considering its unique advantages and current limitations, we identify structural repair, solid-state material recycling, and cladding as the niche engineering applications for AFSD. We point out the research needs to better understand the process fundamentals, especially the physics underlying material deformation and flow, heat generation, temperature evolution, and the coupling of the thermal and deformation history. We also call the readers' attention to the potential of unlocking new opportunities for material innovation across multiple length scales using AFSD.

Looking ahead, because of its unmatched capabilities of rendering excellent mechanical properties, we argue that AFSD can grow into a dominant additive manufacturing solution for the aerospace, automotive, and defense industries where load-bearing capacity is critical. From a material research perspective, AFSD offers ample space for innovation as it can simultaneously control the macrostructure (i.e. shape), mesostructure, and microstructure of a component. Integration of AFSD with existing or emerging topics, such as lightweight metals, nanostructured

materials, high entropy alloys, heterogeneous materials may lead to the next wave of research in the metallurgy community.

Acknowledgement

The authors would like to acknowledge the financial support from the US Army Research Laboratory (W911NF1920320 for HZY and W911NF1920011 for RSM). HZY would like to thank Ryan Gottwald for helpful comments and assistance in figure preparation.

Disclosure statement

No potential conflict of interest was reported by the author(s).

Funding

The authors would like to acknowledge the financial support from the Army Research Laboratory (W911NF1920320 for HZY and W911NF1920011 for RSM).

ORCID

Hang Z. Yu  <http://orcid.org/0000-0002-7629-9577>

Rajiv S. Mishra  <http://orcid.org/0000-0002-1699-0614>

References

- [1] Viswanathan S. ASM International. Handbook committee: casting. Materials Park (OH): ASM International; 2008.
- [2] Semiatin SL. ASM International. Handbook Committee, Metalworking: sheet forming. Materials Park (OH): ASM International; 2006.
- [3] Tarng YS, Juang SC, Chang CH. The use of grey-based Taguchi methods to determine submerged arc welding process parameters in hardfacing. *J Mater Process Technol.* 2002;128(1–3):1–6.
- [4] Juang SC, Tarng YS. Process parameter selection for optimizing the weld pool geometry in the tungsten inert gas welding of stainless steel. *J Mater Process Technol.* 2002;122(1):33–37.
- [5] Aslanlar S. The effect of nucleus size on mechanical properties in electrical resistance spot welding of sheets used in automotive industry. *Mater Des.* 2006;27(2):125–131.
- [6] Benyounis KY, Olabi AG, Hashmi MSJ. Effect of laser welding parameters on the heat input and weld-bead profile. *J Mater Process Technol.* 2005;164:978–985.
- [7] Cornu J. Fundamentals of fusion welding technology, IFS. Bedford (UK); Berlin (NY): Springer; 1988.
- [8] Lippold JC, Kotecki DJ. Welding metallurgy and weldability of stainless steels. Hoboken (NJ): Wiley-Interscience; 2005.
- [9] Dietrich D, Nickel D, Krause M, et al. Formation of intermetallic phases in diffusion-welded joints of aluminium and magnesium alloys. *J Mater Sci.* 2011;46(2):357–364.
- [10] Bakavos D, Prangnell PB. Mechanisms of joint and microstructure formation in high power ultrasonic spot welding 6111 aluminium automotive sheet. *Mater Sci Eng A.* 2010;527(23):6320–6334.
- [11] Carpenter SH, Wittman RH. Explosion welding. *Annu Rev Mater Sci.* 1975;5:177–199.
- [12] Findik F. Recent developments in explosive welding. *Mater Des.* 2011;32(3):1081–1093.
- [13] Akinlabi ET, Mahamood RM. Solid-state welding friction and friction stir welding processes, mechanical engineering. Cham: Springer; 2020. p. 1. online resource (p. 157).
- [14] American Society for Metals. Joining Division, ASM International. Handbook Committee, Welding fundamentals and processes. Materials Park (OH): ASM International; 2011.
- [15] Gibson I, Rosen D, Stucker B. Additive manufacturing technologies: 3D printing, rapid prototyping, and direct digital manufacturing. New York (NY): Springer; 2015. p. 1. online resource (xxi, p. 498).
- [16] Frazier WE. Metal additive manufacturing: a review. *J Mater Eng Perform.* 2014;23(6):1917–1928.
- [17] Sames WJ, List FA, Pannala S, et al. The metallurgy and processing science of metal additive manufacturing. *Int Mater Rev.* 2016;61(5):315–360.
- [18] Everton SK, Hirsch M, Stravroulakis P, et al. Review of in-situ process monitoring and in-situ metrology for metal additive manufacturing. *Mater Des.* 2016;95:431–445.
- [19] Lewandowski JJ, Seifi M. Metal additive manufacturing: a review of mechanical properties. *Annu Rev Mater Res.* 2016;46:151–186.
- [20] DeRoy T, Mukherjee T, Wei HL, et al. Metallurgy, mechanistic models and machine learning in metal printing. *Nat Rev Mater.* 2020. DOI:10.1038/s41578-020-00236-1.
- [21] Basak A, Das S. Epitaxy and microstructure evolution in metal additive manufacturing. *Annu Rev Mater Res.* 2016;46:125–149.
- [22] Martin JH, Yahata BD, Hundley JM, et al. 3D printing of high-strength aluminium alloys. *Nature.* 2017;549(7672):365–369.
- [23] Li N, Huang S, Zhang GD, et al. Progress in additive manufacturing on new materials: a review. *J Mater Sci Technol.* 2019;35(2):242–269.
- [24] Zhang JL, Song B, Wei QS, et al. A review of selective laser melting of aluminum alloys: processing, microstructure, property and developing trends. *J Mater Sci Technol.* 2019;35(2):270–284.
- [25] Tuncer N, Bose A. Solid-state metal additive manufacturing: a review. *JOM.* 2020;72:3090–3111.
- [26] Dehoff RR, Babu SS. Characterization of interfacial microstructures in 3003 aluminum alloy blocks fabricated by ultrasonic additive manufacturing. *Acta Mater.* 2010;58(13):4305–4315.
- [27] Hehr A, Norfolk M. A comprehensive review of ultrasonic additive manufacturing. *Rapid Prototyp J.* 2019;26(3):445–458.
- [28] Assadi H, Kreye H, Gartner F, et al. Cold spraying—a materials perspective. *Acta Mater.* 2016;116:382–407.
- [29] Yin S, Cavaliere P, Aldwell B, et al. Cold spray additive manufacturing and repair: fundamentals and applications. *Addit Manuf.* 2018;21:628–650.
- [30] Yu HZ, Jones ME, Brady GW, et al. Non-beam-based metal additive manufacturing enabled by additive friction stir deposition. *Scr Mater.* 2018;153:122–130.

- [31] Phillips BJ, Avery DZ, Liu T, et al. Microstructure-deformation relationship of additive friction stir-deposition Al–Mg–Si. *Materialia*. 2019;7:100387.
- [32] Chen CY, Xie YC, Yan XC, et al. Effect of hot isostatic pressing (HIP) on microstructure and mechanical properties of Ti6Al4V alloy fabricated by cold spray additive manufacturing. *Addit Manuf*. 2019;27:595–605.
- [33] Wang X, Feng F, Klecka MA, et al. Characterization and modeling of the bonding process in cold spray additive manufacturing. *Addit Manuf*. 2015;8:149–162.
- [34] Griffiths RJ, Perry MEJ, Sietins JM, et al. A perspective on solid-state additive manufacturing of aluminum matrix composites using MELD. *J Mater Eng Perform*. 2019;28(2):648–656.
- [35] Rivera OG, Allison PG, Jordon JB, et al. Microstructures and mechanical behavior of Inconel 625 fabricated by solid-state additive manufacturing. *Mater Sci Eng A*. 2017;694:1–9.
- [36] Perry MEJ, Griffiths RJ, Garcia D, et al. Morphological and microstructural investigation of the non-planar interface formed in solid-state metal additive manufacturing by additive friction stir deposition. *Addit Manuf*. 2020;35:101293.
- [37] Jordon JB, Allison PG, Phillips BJ, et al. Direct recycling of machine chips through a novel solid-state additive manufacturing process. *Mater Des*. 2020;193:108850.
- [38] Kobryn PA, Moore EH, Semiati SL. The effect of laser power and traverse speed on microstructure, porosity, and build height in laser-deposited Ti-6Al-4V. *Scr Mater*. 2000;43(4):299–305.
- [39] Mukherjee T, DebRoy T. Mitigation of lack of fusion defects in powder bed fusion additive manufacturing. *J Manuf Process*. 2018;36:442–449.
- [40] Gunenthiram V, Peyre P, Schneider M, et al. Experimental analysis of spatter generation and melt-pool behavior during the powder bed laser beam melting process. *J Mater Process Technol*. 2018;251:376–386.
- [41] Iebba M, Astarita A, Mistretta D, et al. Influence of powder characteristics on formation of porosity in additive manufacturing of Ti-6Al-4V components. *J Mater Eng Perform*. 2017;26(8):4138–4147.
- [42] Wei HL, Mazumder J, DebRoy T. Evolution of solidification texture during additive manufacturing. *Sci Rep*. 2015;5(1):16446.
- [43] Popovich VA, Borisov EV, Popovich AA, et al. Functionally graded Inconel 718 processed by additive manufacturing: crystallographic texture, anisotropy of microstructure and mechanical properties. *Mater Des*. 2017;114:441–449.
- [44] Dehoff RR, Kirka MM, Sames WJ, et al. Site specific control of crystallographic grain orientation through electron beam additive manufacturing. *Mater Sci Technol*. 2015;31(8):931–938.
- [45] Bermingham MJ, StJohn DH, Krynen J, et al. Promoting the columnar to equiaxed transition and grain refinement of titanium alloys during additive manufacturing. *Acta Mater*. 2019;168:261–274.
- [46] Liu P, Wang Z, Xiao Y, et al. Insight into the mechanisms of columnar to equiaxed grain transition during metallic additive manufacturing. *Addit Manuf*. 2019;26:22–29.
- [47] Lin T-C, Cao C, Sokoluk M, et al. Aluminum with dispersed nanoparticles by laser additive manufacturing. *Nat Commun*. 2019;10(1):4124.
- [48] Li R, Wang M, Li Z, et al. Developing a high-strength Al-Mg-Si-Sc-Zr alloy for selective laser melting: crack-inhibiting and multiple strengthening mechanisms. *Acta Mater*. 2020;193:83–98.
- [49] Avery DZ, Phillips BJ, Mason CJT, et al. Influence of grain refinement and microstructure on fatigue behavior for solid-state additively manufactured Al-Zn-Mg-Cu Alloy. *Metall Mater Trans A*. 2020;51(6):2778–2795.
- [50] Garcia D, Hartley WD, Rauch HA, et al. In situ investigation into temperature evolution and heat generation during additive friction stir deposition: a comparative study of Cu and Al-Mg-Si. *Addit Manuf*. 2020;34:101386.
- [51] McNelley TR, Swaminathan S, Su JQ. Recrystallization mechanisms during friction stir welding/processing of aluminum alloys. *Scr Mater*. 2008;58(5):349–354.
- [52] Humphreys FJ, Hatherly M. Recrystallization and related annealing phenomena. 2nd ed. Amsterdam; Boston: Elsevier; 2004.
- [53] Sakai T, Belyakov A, Kaibyshev R, et al. Dynamic and post-dynamic recrystallization under hot, cold and severe plastic deformation conditions. *Prog Mater Sci*. 2014;60:130–207.
- [54] Huang K, Logé RE. A review of dynamic recrystallization phenomena in metallic materials. *Mater Des*. 2016;111:548–574.
- [55] Rivera OG, Allison PG, Brewer LN, et al. Influence of texture and grain refinement on the mechanical behavior of AA2219 fabricated by high shear solid state material deposition. *Mater Sci Eng A*. 2018;724:547–558.
- [56] Griffiths RJ, Petersen DT, Garcia D, et al. Additive friction stir-enabled solid-state additive manufacturing for the repair of 7075 aluminum alloy. *Appl Sci*. 2019;9(17):3486.
- [57] Liu ZY, Li C, Fang XY, et al. Energy consumption in additive manufacturing of metal parts. *Procedia Manuf*. 2018;26:834–845.
- [58] Agrawal R, Vinodh S. State of art review on sustainable additive manufacturing. *Rapid Prototyp J*. 2019;25(6):1045–1060.
- [59] Tillmann W, Schaak C, Nellesen J, et al. Hot isostatic pressing of IN718 components manufactured by selective laser melting. *Addit Manuf*. 2017;13:93–102.
- [60] Qian M, Xu W, Brandt M, et al. Additive manufacturing and postprocessing of Ti-6Al-4V for superior mechanical properties. *MRS Bull*. 2016;41(10):775–784.
- [61] Editors DE. MELD prints 10-foot Aluminum cylinder, digital engineering. 2020. Available from: <https://www.digitalengineering247.com/article/meld-prints-10-foot-aluminum-cylinder/>.
- [62] Hartley WD, Garcia D, Yoder JK, et al. Solid-state cladding on thin automotive sheet metals Enabled by additive friction stir deposition. *J Mater Process Technol Under Rev*. 2020.
- [63] Mishra RS, De PS, Kumar N. Friction stir welding and processing: science and engineering. Cham: Springer; 2014, p. 1 online resource (xii, p. 338).
- [64] Nandan R, Roy GG, Lienert TJ, et al. Three-dimensional heat and material flow during friction stir welding of mild steel. *Acta Mater*. 2007;55(3):883–895.
- [65] Liu XC, Sun YF, Nagira T, et al. Experimental evaluation of strain and strain rate during rapid cooling friction stir welding of pure copper. *Sci Technol Weld Joining*. 2019;24(4):352–359.

- [66] Cunningham R, Zhao C, Parab N, et al. Keyhole threshold and morphology in laser melting revealed by ultrahigh-speed x-ray imaging. *Science*. 2019;363(6429):849–852.
- [67] Kumar R, Pancholi V, Bharti RP. Material flow visualization and determination of strain rate during friction stir welding. *J Mater Process Technol*. 2018;255:470–476.
- [68] De PS, Mishra RS, Smith CB. Effect of microstructure on fatigue life and fracture morphology in an aluminum alloy. *Scr Mater*. 2009;60(7):500–503.
- [69] Sharma SR, Ma ZY, Mishra RS. Effect of friction stir processing on fatigue behavior of A356 alloy. *Scr Mater*. 2004;51(3):237–241.
- [70] Meyers MA, Mishra A, Benson DJ. Mechanical properties of nanocrystalline materials. *Prog Mater Sci*. 2006;51(4):427–556.
- [71] Sinha S, Mirshams RA, Wang T, et al. Nanoindentation behavior of high entropy alloys with transformation-induced plasticity. *Sci Rep*. 2019;9(1):6639.
- [72] Nene SS, Liu K, Frank M, et al. Enhanced strength and ductility in a friction stir processing engineered dual phase high entropy alloy. *Sci Rep*. 2017;7:7.
- [73] Gourdet S, Montheillet F. A model of continuous dynamic recrystallization. *Acta Mater*. 2003;51(9):2685–2699.
- [74] Baczynski J, Jonas JJ. Torsion textures produced by dynamic recrystallization in α -iron and two interstitial-free steels. *Metall Mater Trans A*. 1998;29(2):447–462.
- [75] Barr CM, Thomas S, Hart JL, et al. Tracking the evolution of intergranular corrosion through twin-related domains in grain boundary networks. *npj Mater Degrad*. 2018;2(1):14.
- [76] Bechtle S, Kumar M, Somerday BP, et al. Grain-boundary engineering markedly reduces susceptibility to intergranular hydrogen embrittlement in metallic materials. *Acta Mater*. 2009;57(14):4148–4157.
- [77] Fan XH, Li M, Li DY, et al. Dynamic recrystallisation and dynamic precipitation in AA6061 aluminium alloy during hot deformation. *Mater Sci Technol*. 2014;30(11):1263–1272.
- [78] Ma XL, Eswarappa Pameela S, Yi P, et al. Dynamic precipitation and recrystallization in Mg-9wt.%Al during equal-channel angular extrusion: a comparative study to conventional aging. *Acta Mater*. 2019;172:185–199.
- [79] Chen YC, Feng JC, Liu HJ. Precipitate evolution in friction stir welding of 2219-T6 aluminum alloys. *Mater Charact*. 2009;60(6):476–481.
- [80] Huang K, Marthinsen K, Zhao Q, et al. The double-edge effect of second-phase particles on the recrystallization behaviour and associated mechanical properties of metallic materials. *Prog Mater Sci*. 2018;92:284–359.
- [81] Dogan E, Wang S, Vaughan MW, et al. Dynamic precipitation in Mg-3Al-1Zn alloy during different plastic deformation modes. *Acta Mater*. 2016;116:1–13.
- [82] Palanivel S, Nelaturu P, Glass B, et al. Friction stir additive manufacturing for high structural performance through microstructural control in an Mg based WE43 alloy. *Mater Des*. 2015;65:934–952.
- [83] Panigrahi SK, Mishra RS, Brennan RC, et al. Achieving extraordinary structural efficiency in a wrought magnesium rare earth alloy. *Mater Res Lett*. 2020;8(4):151–157.
- [84] Dutt AK, Gwalani B, Tungala V, et al. A novel nanoparticle strengthened titanium alloy with exceptional specific strength. *Sci Rep*. 2019;9:11726. DOI:10.1038/s41598-019-48139-8.
- [85] Mironov S, Sato YS, Kokawa H. Friction-stir welding and processing of Ti-6Al-4V titanium alloy: a review. *J Mater Sci Technol*. 2018;34(1):58–72.
- [86] Hanamura T, Yin F, Nagai K. Ductile-brittle transition temperature of ultrafine Ferrite/cementite microstructure in a low carbon steel controlled by effective grain size. *ISIJ Int*. 2004;44(3):610–617.
- [87] Sekban DM, Aktarer SM, Xue P, et al. Impact toughness of friction stir processed low carbon steel used in shipbuilding. *Mater Sci Eng A*. 2016;672:40–48.
- [88] Huang M, Rivera-Díaz-del-Castillo PEJ, Bouaziz O, et al. Modelling strength and ductility of ultrafine grained BCC and FCC alloys using irreversible thermodynamics. *Mater Sci Technol*. 2009;25(7):833–839.
- [89] Koch CC. Optimization of strength and ductility in nanocrystalline and ultrafine grained metals. *Scr Mater*. 2003;49(7):657–662.
- [90] Ma E, Wu X. Tailoring heterogeneities in high-entropy alloys to promote strength–ductility synergy. *Nat Commun*. 2019;10(1):5623.
- [91] Miyamoto Y. Functionally graded materials: design, processing, and applications. Boston: Kluwer Academic Publishers; 1999.
- [92] Kieback B, Neubrand A, Riedel H. Processing techniques for functionally graded materials. *Mater Sci Eng A*. 2003;362(1):81–106.
- [93] Eizadjou M, Kazemi Talachi A, Danesh Manesh H, et al. Investigation of structure and mechanical properties of multi-layered Al/Cu composite produced by accumulative roll bonding (ARB) process. *Compos Sci Technol*. 2008;68(9):2003–2009.
- [94] Saito Y, Utsunomiya H, Tsuji N, et al. Novel ultra-high straining process for bulk materials—development of the accumulative roll-bonding (ARB) process. *Acta Mater*. 1999;47(2):579–583.
- [95] Duchaussoy A, Sauvage X, Edalati K, et al. Structure and mechanical behavior of ultrafine-grained aluminum-iron alloy stabilized by nanoscaled intermetallic particles. *Acta Mater*. 2019;167:89–102.
- [96] Hannard F, Castin S, Maire E, et al. Ductilization of aluminium alloy 6056 by friction stir processing. *Acta Mater*. 2017;130:121–136.
- [97] Wu X, Zhu Y. Heterogeneous materials: a new class of materials with unprecedented mechanical properties. *Mater Res Lett*. 2017;5(8):527–532.
- [98] Ma E, Zhu T. Towards strength–ductility synergy through the design of heterogeneous nanostructures in metals. *Mater Today*. 2017;20(6):323–331.
- [99] Zhu Y, Wu X. Perspective on hetero-deformation induced (HDI) hardening and back stress. *Mater Res Lett*. 2019;7(10):393–398.
- [100] Estrin Y, Beygelzimer Y, Kulagin R. Design of architected materials based on mechanically driven structural and compositional patterning. *Adv Eng Mater*. 2019;21(9):1900487.